RESEARCH ARTICLE

Non-invasive characterization of different types of basal cell carcinomas (BCCs) using vibrational optical coherence tomography (VOCT): Can early lesions as small as 0.05 mm be identified by VOCT?

Authors
Frederick H. Silver[1,2], Tanmay Deshmukh[2], Nicole Ryan[3], Arielle Romm[3], and Hari Nadiminti[3]

Affiliations
[1] Department of Pathology and Laboratory Medicine, Robert Wood Johnson Medical School, Rutgers, the State University of New Jersey, Piscataway, NJ 08854
[2] OptoVibronex, LLC., Allentown, PA
[3] Dermatology, Summit Health, Berkeley Heights NJ 07922

Corresponding author:
Frederick H. Silver
Email: fhsilver@hotmail.com

Abstract
Vibrational optical coherence tomography (VOCT) has been used to non-invasively measure the resonant frequency and elastic modulus of different types of BCCs to compare the physical biomarker characteristics of each of these lesions. The results suggest that in very small lesions (about 0.05 mm in diameter) new 80Hz and 130Hz resonant frequency peaks are seen not present in normal skin or in healing wounds. In all other BCCs, new 80Hz, 130Hz and 260Hz resonant frequency peaks are found like those found in other carcinomas including SCC and melanoma.
Small BCCS are characterized by new 80Hz and 130Hz in the absence of a significant 50Hz peak unlike actinic keratoses that are characterized by 50Hz, 80Hz and 130Hz peaks. In the absence of the 260Hz peak, small BCCs appear to be a precursor to larger BCCs. Pigmented BCCs exhibit a larger ratio of the 50Hz/80Hz peaks compared to the other BCC types in addition to peaks at 130Hz and 260Hz suggesting that benign melanocyte lesions contribute to the 50 Hz peak. Further studies are needed to understand the factors that drive differences in shape and invasiveness of cancerous BCCs.
While all BCCs were found to contain new cell and blood vessel resonant frequencies that coincide with fibrotic tissue encapsulating the tumors in the papillary dermis, other factors must drive differences in the shape and invasiveness of the different BCCs. It is hypothesized that the new cells and blood vessels formed lead to the deposition of fibrous tissue in all BCCs and is partially driven by an epithelial-mesenchyme transition. It is concluded that fibrotic tissue is found encapsulating all cancerous BCCs and that this layer of tissue may limit invasiveness and metastatic behavior of this tumor type. In general, tumor shape and invasiveness are likely influenced by the exact cellular mutations in each lesion type and the extent of UV light damage experienced by the surrounding extracellular matrix.

1.0 Introduction

Basal cell carcinoma (BCC) is the most prevalent form of skin cancer worldwide. It accounts for 90% of all the skin cancers in the United States [1-4]. By 2050 it is predicted that there will be almost 50 million skin biopsies performed in the US each year [1-4]. This will overload the health care system especially if the number of skin biopsies done each year continues to be about twice the number of skin cancers diagnosed [5].

Basal cell carcinoma has an overall incidence that is increasing worldwide by 3-10% each year, especially in young women [6]. Like melanoma and SCC, the pathogenesis of BCC involves cumulative and intermittent exposure to ultraviolet (UV) radiation, particularly the ultraviolet B spectrum (290-320nm) [7]. Malignant activation of the sonic hedgehog (SHH) signaling pathway is well known as a key feature of BCC and therefore it is a therapeutic target for treatment. The most common genes mutated in sporadic basal cell carcinoma are: PTCH1 (73%), SMO, and SUFU [8]. Basal cell carcinomas show a wide spectrum of dermoscopic features [9]. However, most of these lesions do not form secondary tumors and therefore are a good model of a “stable” cancer.

There are four classifications of BCCs including nodular, superficial, sclerosing and pigmented basal cell carcinomas [10]. While there are four major classifications that are used in pathological analysis of these tumors, there are few quantitative studies on the composition of these subtypes.

The predominant form is nodular BCC that accounts for 50% of these lesions; it is histologically characterized by aggregates of basaloid cells with well-defined borders. These well-defined borders appear to contain extracellular matrix (ECM) with prominent vessels [11-13] and collagen [14].

Pigmentation can be found in different clinical versions of basal cell carcinoma including nodular, micronodular, multifocal and superficial BCC, and the color of these lesions can vary. Histological study results on pigmented BCC show nests of basaloid cells, abundance of melanin and melanophages, and a moderate inflammatory infiltrate [10].

Superficial BCC is another common variant of BCC. It is characterized by nests of basaloid cells that extend from the epidermis, with neoplastic cells that resemble primordial germ cells. Peripheral palisading is usually prominent and tumor islands show a well demarcated border [15]. Sclerosing BCC presents histologically as nests and clusters of tumor cells that are surrounded by thick fibrotic stroma. Clinically, it is presented as infiltrated plaque with slightly shining surface and indistinct borders [10].

Much of the literature focuses on the different forms of BCC and their diagnosis by visual and dermoscopic evaluation. However, due to the increasing numbers of BCCs observed in the clinic, it is essential to develop additional screening techniques for early diagnosis of these lesions. Also, there is a need to identify difficult lesions early, especially on the head, face, nose, and neck, to limit the need for extensive cosmetic reconstruction after lesion excision. The existence of a technique to diagnose early BCCs and their major components would be an important step in understanding the pathogenesis of basal cell carcinoma as well as to develop other therapeutic means for treatment. If an early BCC lesion can be identified, then it may be possible to develop topical skin treatments to slow the invasiveness or eliminate these lesions before they grow further.

Recently we reported the results of studies involving use of vibrational optical coherence tomography (VOCT) to study the stiffness of

the components of normal skin, actinic keratosis, BCC, squamous cell carcinoma (SCC), and melanoma [15-17]. The technique uses audible sound and infrared light to non-invasively measure the resonant frequency of skin components and then convert the measurements into a stiffness (modulus) map for each of these lesions [17]. The results of these studies suggest that the location and physical biomarker characteristics of skin cancers are different than those found in normal skin and benign lesions and can be identified virtually using VOCT [15-17]. Benign skin lesions have major peaks at 50Hz (normal cells), 150Hz (normal blood vessels) and 100Hz (dermal collagen) [15]. Pre-cancerous actinic keratosis (AK) has additional peaks at 80 Hz (new epidermally derived cells) and 130Hz (new blood vessels), and cancerous lesions (BCC, SCC and melanoma) have peaks at 80Hz, 130Hz and 260Hz (new fibrotic tissue) (15-17).

3D images created based on changes in cellular and fibrous tissue stiffness along with changes in vascular quality can be used to map and evaluate different types of cancers including melanoma (17). While VOCT cannot identify changes at the cellular level, it can quantitatively identify the new vessel and fibrous tissue deposition that are associated with different cancers and it can be used to differentiate between melanomas and other cancerous lesions (17). 3D tumor maps constructed from VOCT data and the location and the heights of the 80, 130 and 260 Hz peaks can be created prior to surgery from non-invasive measurements. These measurements can be made directly on the patient and be used to plan the removal of difficult skin lesions using telemedicine conferences, where extensive surgery may be needed to remove the entire tumor in one step. The purpose of this paper is to present images and quantitative VOCT data to compare the four subtypes of BCC non-invasively. The results presented suggest that all the subtypes have similar changes in the resonant frequency and stiffness (modulus) of the cells, blood vessels and fibrotic tissue. It is further hypothesized that like in actinic keratosis, changes in the resonant frequency of cells and blood vessels precede large scale deposition of fibrotic tissue with a resonant frequency of 260 Hz. This change is a sign of tumor invasiveness. Finally, it is shown that small BCC lesions appear to be characterized by the 80Hz and 130Hz peaks and lack the large fibrotic peak at 260Hz. The presence of 80Hz and 130Hz peaks and the lack of the fibrotic peak at 260Hz may be a sign of early cancer formation.

2.0 Methods

2.1 Subjects

Normal skin from 14 subjects (11 males and 3 females) was studied *in vivo* using VOCT after informed consent was obtained as reported previously [16,17]. Control skin was examined from the hands, arms and legs of each subject. The resonant frequencies of the components of skin were measured *in vivo* by mounting the OCT hand piece on a custom-built universal mount that was supported over the area of skin to be studied [15-17]. The subjects studied ranged in age from 21 to 71 years old.

Suspicious skin lesions identified by dermoscopy in the Dermatology Clinic at Summit Health (Berkeley Heights, NJ) were biopsied and studied *in vitro* using VOCT on a sample stand [17,18]. These lesions appeared during dermoscopic examination to contain layers of cells, superficial blood vessels or abnormal color. They were obtained from the arms, back, legs, abdomen and necks of subjects at Summit Health. The biopsied lesions were studied blindly by VOCT without identification of the age and sex of the patient. Forty biopsies of complete excisions and fifty-one Mohs sections were examined using VOCT as part of an IRB approved study.

Several of the biopsies were large enough to make multiple measurements on different areas of each sample. VOCT measurements were made on areas of about 0.0625 mm^2. All subjects signed consent forms prior to enrolling in the study.

2.2 OCT Images and Scans of Pixel Intensity Versus Depth

OCT image collection was accomplished using a Lumedica Spectral Domain OQ 2.0 Labscope (Lumedica Inc., Durham, NC) operating in the scanning mode at a wavelength of 840nm. The device generates a 512 x 512 pixel image with a transverse resolution of 15 micrometers and an A-scan rate of 13,000/sec. All gray scale OCT images were color coded to enhance the image details. For the pixel intensity versus depth plots, the surface of the sample was electronically traced and the averages of pixel values were calculated along the surface of the sample, which were then plotted against the depth. For curved biopsy specimen, the tracing was done parallel to the surface of the image.

Multiple cross-sectional OCT scans were collected using the volume scan software included in the Lumedica OQ Labscope and processed into 3D images using image J software.

The pixel intensities obtained from the gray scale images were plotted versus depth for each sample studied. The enhanced OCT images used darker colored (blue and purple) regions to reflect lower pixel intensities while the lighter (yellowish) regions reflected higher pixel intensity regions. Pixel intensities were processed using image J software, analyzed with a MATLAB program, and plotted versus skin depth. Previous studies have shown that the images of normal skin and cancerous lesions seen by OCT correlate with the histological images seen in sections cut from tissue biopsies [18,19].

2.3 Measurement of Resonant Frequency and the Elastic Modulus

The OQ Labscope was modified by adding a 2 inch diameter speaker to vibrate the tissue in the VOCT studies [16,17]. The Labscope was also modified to collect and store single raw image data that was used to calculate sample displacements (amplitude information) from A line data. The data was processed using MATLAB software as discussed previously [20-24]. The displacement of the tissue is detected by measuring the frequency dependence of the deformation based on the reflected infrared light and filtered to collect only vibrations that were in phase (elastic component) with the sound input signal. The vibrations for each frequency were isolated to calculate the amplitude. These amplitudes were plotted against the frequency of the vibrations. The result is a spectrum of displacements for specific tissue components as a function of frequency of the applied sound; the resonant frequency of each tissue component, e.g. cells (50-80Hz), dermal collagen (100Hz-120), blood vessels (130-150Hz) and fibrotic tissue (180-260Hz), have been assigned previously based on studies on a variety of soft tissues and polymeric materials [20-26].

The resonant frequency of a tissue component is defined as the frequency at which the maximum in-phase displacement is observed in the amplitude data for that component. The measured resonant frequencies are converted into elastic modulus values using a calibration equation (equation 1) developed based on *in vitro* uniaxial mechanical tensile testing and VOCT measurements made on the same tissue at the same time as reported previously [20-24]. The resonant frequency of each sample is determined by measuring the displacement of the tissue resulting from transversely applied sinusoidal audible sound driving frequencies ranging from 30 Hz to 300 Hz, in steps of 10 Hz. The peak frequency (the resonant

frequency), f_n, is defined as the frequency at which the displacement is maximized.

Soft Tissues $$E * d = 0.0651 * (fn^2) + 233.16 \quad (1)$$

Calibration studies using *in vitro* uniaxial tensile testing and VOCT measurements were used to develop equation (1) for soft tissues. Since most soft tissues have a density very close to 1.0, equation (1) is valid for most tissues found in the body; where the thickness d is in m and is determined from OCT images, fn^2 is the square of the resonant frequency, and E is the elastic modulus in MPa as discussed previously [20-23] and was used to calculate the modulus values listed in Table 1.

Normal skin studies were conducted *in vivo* using a universal hand piece mount. Tissue biopsies were studied in vitro by VOCT using the microscope stage within 5 minutes of harvesting by the Dermatologist and kept wet using moist saline impregnated gauze during testing.

Once VOCT studies were conducted, the biopsy samples were immersed in fixative and transported to the pathology lab for diagnosis. Histopathology on skin biopsies was conducted by a dermatopathologist after routine dehydration in alcoholic solutions, embedding in paraffin, thin sectioning and staining with H&E. Mohs thin sections were processed after fixation by frozen sectioning and H&E staining. They were reviewed by a trained Mohs dermatopathologist who conducted the pathological analysis.

Table 1. Mean moduli values calculated using equation (1) and standard deviations { } for the resonant frequency peaks found for normal skin, small BCC lesions, nodular BCCs, linear BCCs, sclerosing BCCs, and pigmented BCCs. Note the presence of 80Hz and 130Hz peaks in small BCCs, 80Hz, 130Hz, and 260Hz peaks in all other BCCs.

	No. of measurements	50 Hz	80 Hz	130 Hz	260 Hz
Normal Skin	14	**1.231 {0.140}**	NA	NA	NA
Small BCC	14	1.311 {0.192}	**2.03 {0.34}**	4.19 {0.64}	NA
Nodular BCC	27	**1.467 {0.26}**	2.13 {0.41}	4.41 {0.78}	16.63 {2.62}
Linear BCC	6	1.525 {0.74}	2.27 {0.40}	4.46 {0.69}	16.30 {2.82}
Sclerosing BCC	3	1.329 {0.30}	**3.04 {0.136}**	4.19 {0.53}	15.31 {0.39}
Pigmented BCC	9	1.607 {0.29}	**2.47 {0.52}**	**5.47 {1.048}**	**19 {3.72}**

Values in bold are statistically different at a confidence level of 0.95 or greater. * *t*-Test performed with one-tailed distribution and two-sample unequal variances. NA=not applicable

3.0 Results

A comparison of the biophysical properties of normal skin, nodular BCC, superficial BCC, sclerosing BCC and pigmented BCC was conducted by applying infrared light and audible sound to skin and skin excisions. The VOCT handpiece and speaker are positioned about one inch above the sample to test the tissue non-invasively. While normal skin contains resonant frequency peaks at 50Hz (normal cells), 100 Hz (dermal collagen), 150 Hz (blood vessels), and occasionally small peaks at 180-220Hz (small amounts of fibrous tissue) (Figure 1) all types of BCC lesions had additional peaks. Figure 1 shows 3D OCT image reconstructions of young (A, 26 years

old) and older skin (B, 71 years old). The 3D OCT images show increased wrinkling of the older skin as well as a thicker stratum corneum (yellow) and the 3D plots of weighted displacement versus depth are shown below the 3D images. They illustrate that cells (frequency of 50Hz) are present in the epidermis and papillary dermis at depths up to about 0.4 mm (Figure 1 C and D). Dermal collagen (100Hz) and blood vessels (150Hz) are found in the papillary dermis. Table 1 lists the moduli values for cells and other resonant frequency peaks seen in BCCs. The presence of normal cells, blood vessels and dermal collagen were present in both young and older skin and there did not appear to be large deposits of fibrous tissue with resonant frequencies above 150Hz.

Figure 1

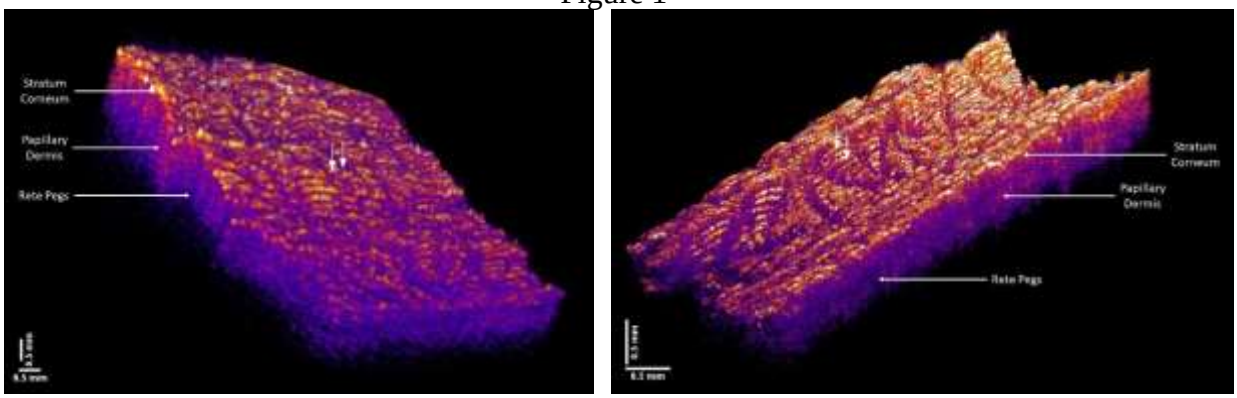

A B

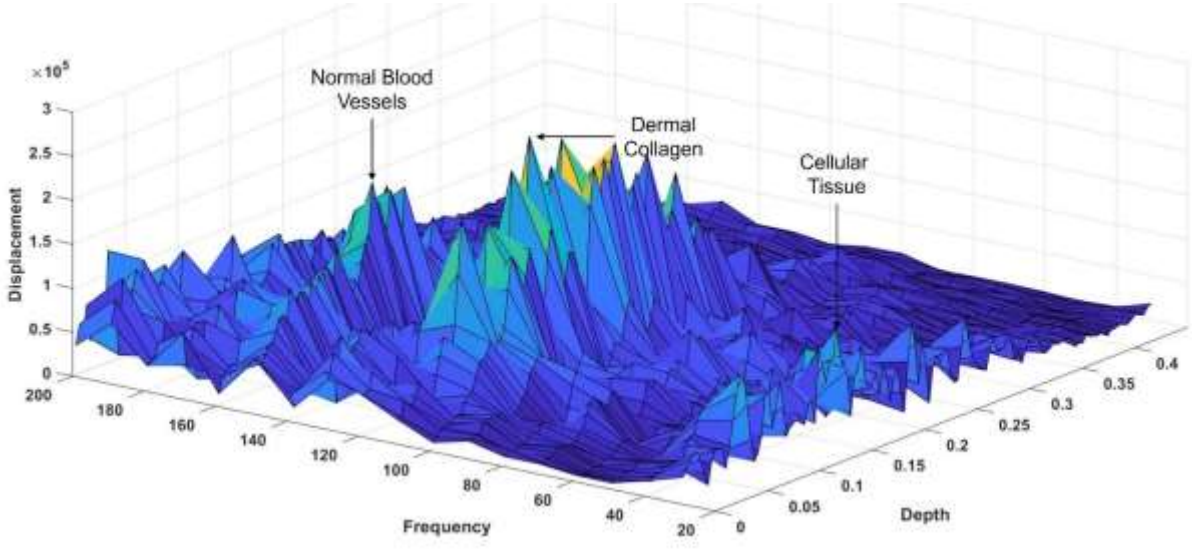

C

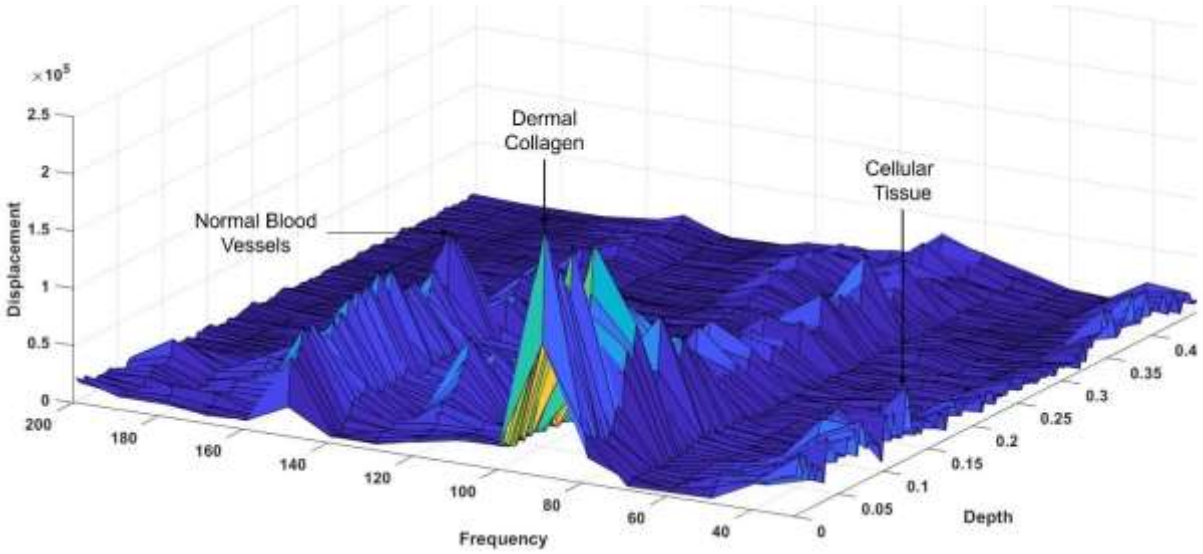

D

Figure 1. Reconstructed 3D color coded OCT image of normal skin from a 26 year old subject (A) and a 71 year old subject (B) illustrating the thicker wrinkled stratum corneum and less apparent rete pegs in the skin from the older subject. 3D plots of the weighted displacement versus frequency and depth of the components of the young (C) and older skin (D) determined from VOCT measurements. Note the peaks at about 50Hz (cells), 100Hz (dermal collagen), and 150 Hz (blood vessels). The cells are found primarily in the epidermis and papillary dermis while the dermal collagen and blood vessels are found in the papillary dermis. White arrows present show the location where the VOCT measurements were made. Magnification bars shown are only an estimate of the dimensions as a result of the 3D perspective of the images shown.

In very small lesions (about 0.05 mm in diameter) in specimen with larger nodular BCC lesions (see Figure 2A, 2C), the resonant frequency peak for normal cells is seen at about 50Hz as well as another new peak at 80Hz that extends from the bottom of the epidermis down to the papillary dermis. Another new peak is seen at 130 Hz in the papillary dermis at a depth of between 0.1 to 0.25 mm. These peaks are similar to those reported previously for actinic keratoses [15-17] and are consistent with a lesion with no large amounts of fibrosis (absence of 260Hz peak). While small lesions did not have a fibrotic peak, they have all the characteristics of a pre-cancer, namely new 80Hz and 130Hz peaks that have been previously assigned to changes in the cells and new friable blood vessels [15-17]. These new peaks have moduli listed in Table 1.

Figure 2

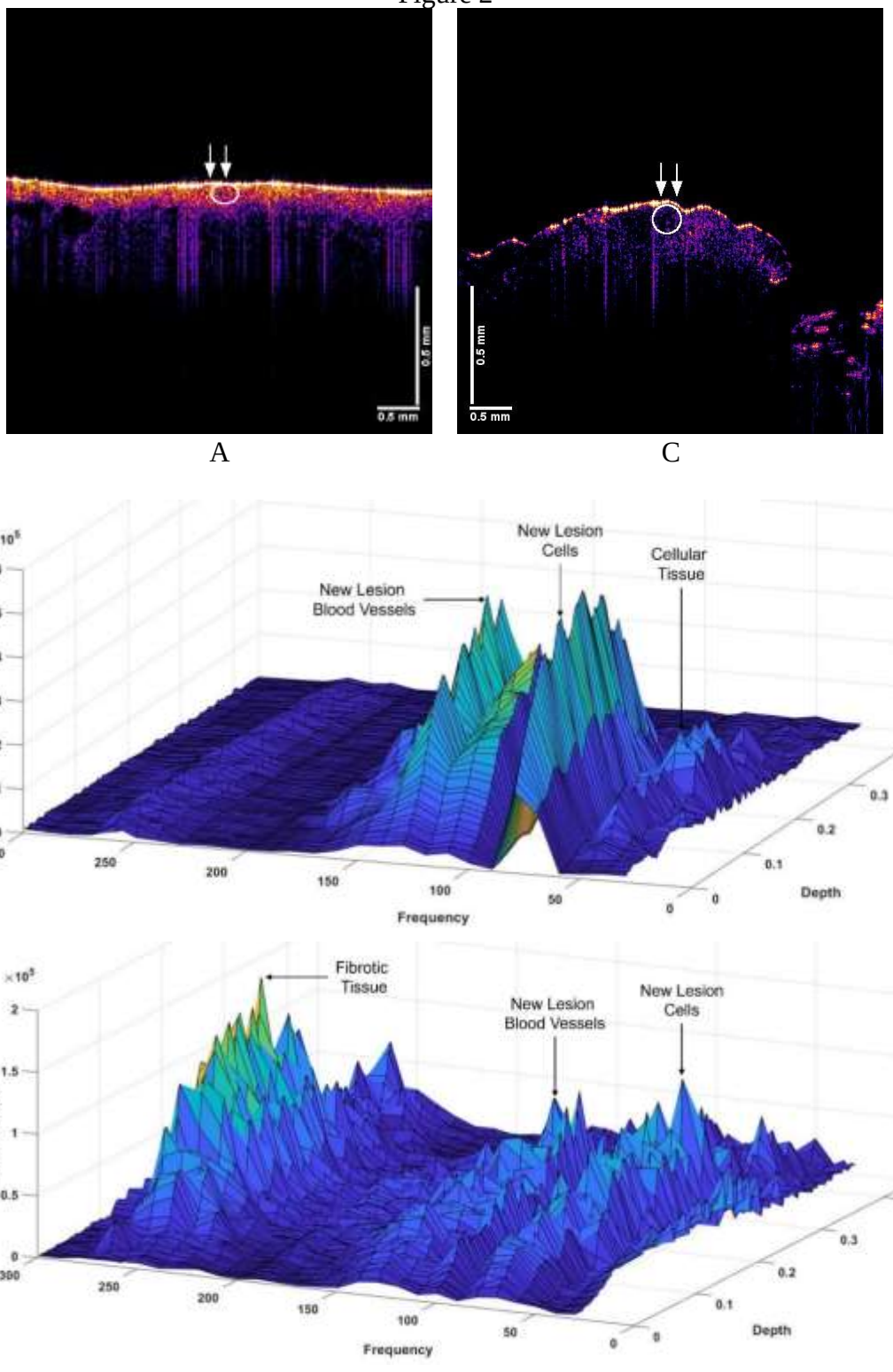

Figure 2. 2D color coded OCT image (A) and VOCT weighted displacement versus frequency versus depth plot (B) for a small lesion near a large nodular BCC (C). Note the small BCC lesions (circles) do not exhibit a large resonant frequency peak at 260Hz (fibrous tissue) in B while the large lesion has a large 260Hz peak

(D). White arrows point to the location where the VOCT measurements were made and the circles indicate where the lesions are found in the image. Note the large black spots in the image surrounding the small lesions are where other large BCC lesions are found.

In larger nodular BCCs (Figure 2B, 2D), with diameters of about 0.33 mm or greater, resonant frequency peaks at 50Hz and 80Hz are present throughout epidermis and papillary dermis, a peak at 130Hz and a new fibrotic peak 260Hz are found in the papillary dermis. These peaks (80Hz, 130Hz and 260Hz) are all characteristic of all skin cancers studied using VOCT including BCC, SCC, and melanoma [15-17]. The relative heights of the 80, 130, and 260Hz peaks are dependent on the type of carcinoma as previously reported [15-17]. The new peak at 80Hz is not seen in healing wounds and the 130Hz peak is absent in wounds after a fibrotic peak at 260Hz forms [21].

Figure 3

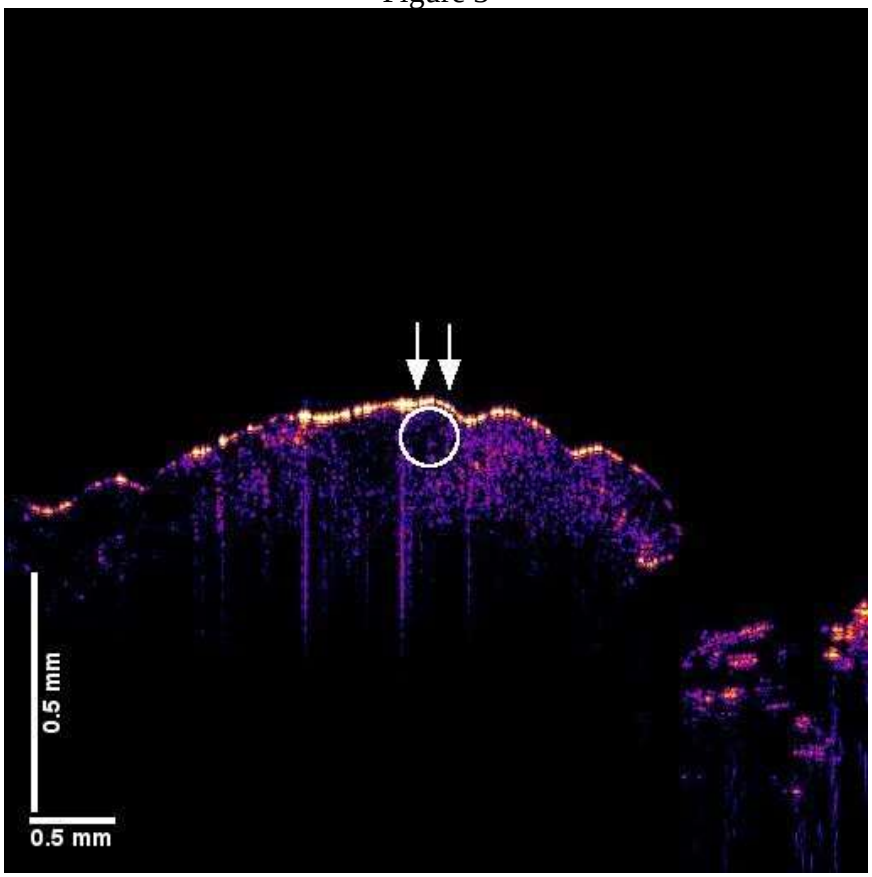

A

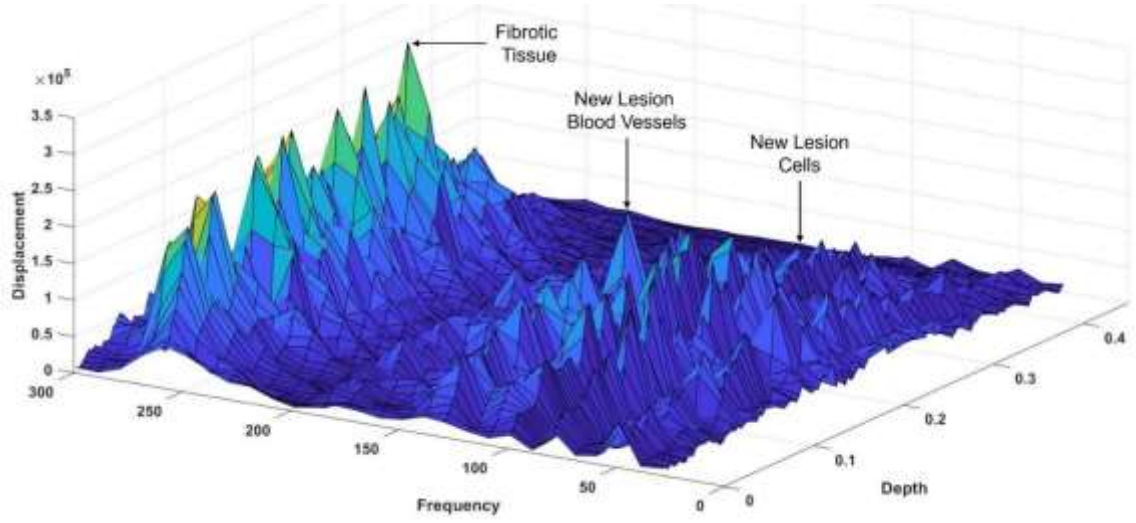

B

Figure 3. 2D color coded OCT image (A) and VOCT weighted displacement versus frequency versus depth plot (B) for a superficial BCC. Note the similarity in the location of the resonant frequency peaks in (3B) to the peaks in the nodular BCC in Figure 2B. All the peak positions are similar in nodular and superficial BCCs. White arrows point to the location where the VOCT measurements were made and the circles indicate where the lesions are found in the image.

Linear BCCs exhibit a similar set of peaks at 50Hz, 80Hz, 130Hz and 260Hz as did nodular BCCs (see Figure 3) and sclerotic BCCs (Figure 4). In contrast, pigmented BCCs have peaks at 50Hz, 80Hz, 130Hz and 260Hz as do the other BCC types, but the 50Hz peak is much larger than the 80Hz peak (Figure 5). In contrast all the other types of BCCs have 50Hz peaks about the same size or smaller than the 80Hz peak (see Figures 2-5). The presence of normal melanocytes appears to increase the size of the 50Hz peak while not altering the presence of the 80, 130 and 260 Hz peaks.

Figure 4

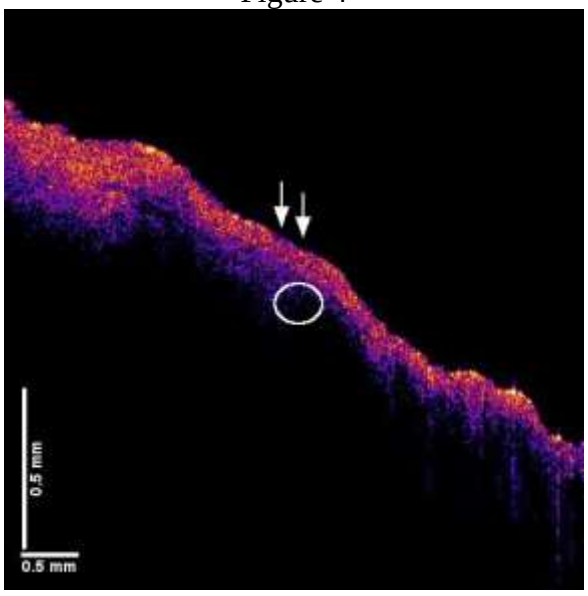

A

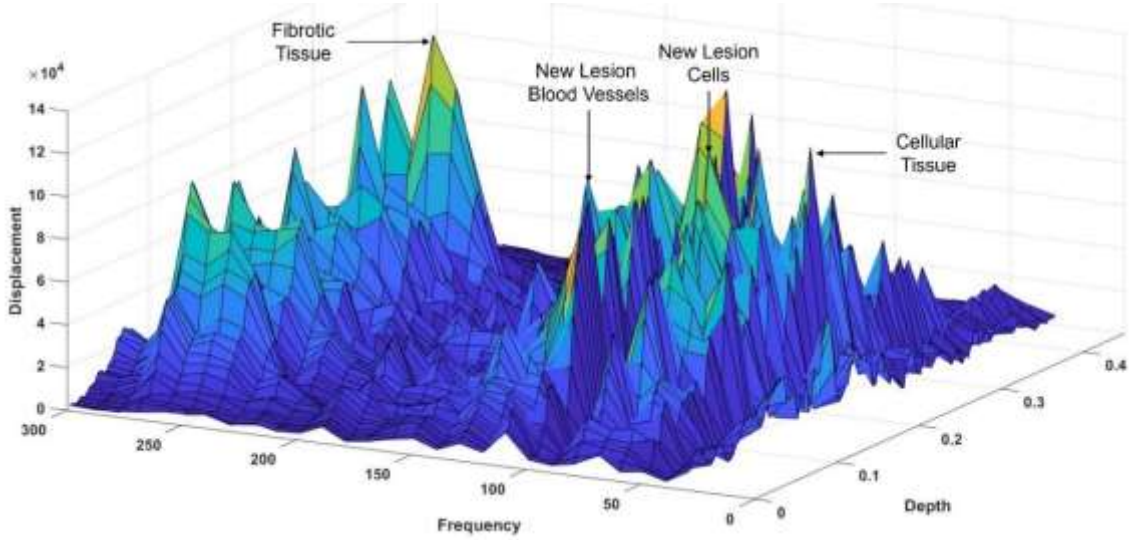

B

Figure 4. 2D color coded OCT image (A) and VOCT weighted displacement versus frequency versus depth plot (B) for a sclerosing BCC. The 3D weighted displacement plots look like plots for nodular and superficial BCC (see Figures 2B and 3B). White arrows show the location where the VOCT measurements were made and the circles indicate where the lesions are found in the image.

Figure 5

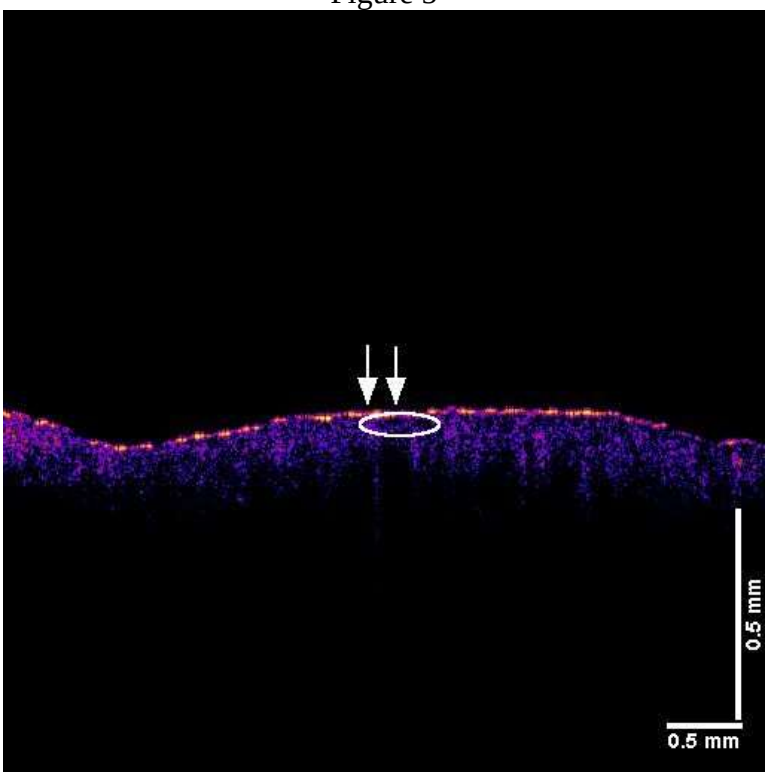

A

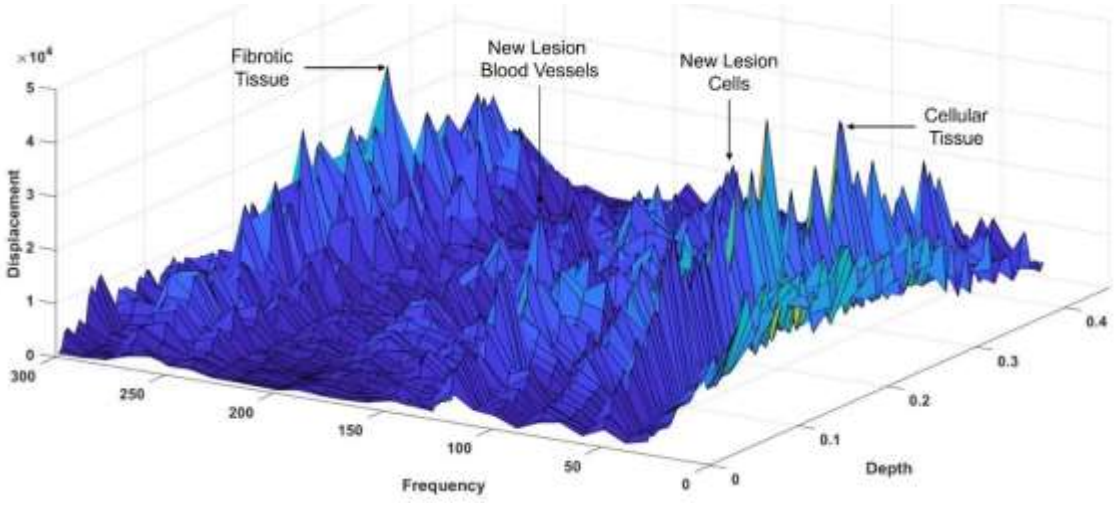

B

Figure 5. 2D color coded OCT image (A) and VOCT weighted displacement versus frequency versus depth plot (B) for a pigmented BCC. Note the increased ratio of the 50/80Hz peak compared to other BCCs seen in Figures 2B, 3B, 4B. White arrows point to the location where the VOCT measurements were made and the circles indicate where the lesions are found in the image.

A comparison of the average 2D plots for the areas studied between the two arrows in the OCT images of weighted displacement versus frequency illustrate the similarity and differences between small lesions in BCC cancers, other BCC lesions, actinic keratoses and pigmented BCCs (Figure 6). While actinic keratoses and small BCC lesions exhibit altered cell and blood vessel physical markers they do not show a dense fibrotic collagen region that is adjacent to the carcinomas. The dense fibrotic tissue peak at 260Hz that is characteristic of all BCC skin carcinomas studied seems to maximize at the same depth as the 80Hz and 130Hz peaks suggesting that the new cells and blood vessels are mixed together with the fibrotic collagen in the tumor.

4.0 Discussion

Although the four different types of BCCs have different morphologies, they all exhibit new resonant frequency peaks at 80Hz, 130Hz and 260Hz characteristic of all cancerous skin lesions (BCC, SCC and melanoma) previously studied by VOCT (15-17). The new 80Hz peak has been hypothesized to reflect cellular changes associated with changes in cell-cell cadherin attachments associated with an epithelial-mesenchymal transition, while the 130Hz peak represents new friable capillaries that are formed because of the epithelial-mesenchymal transition. While the 130Hz peak is seen in healing wounds the 80Hz peak is not present in skin wounds and disappears after the fibrotic peak at 260Hz is formed [15-17]. Formation of these two peaks (80Hz and 130 Hz) appears to occur prior to the deposition of large amounts fibrous tissue in BCC. The 260Hz peak may be driven by release of factors such as TGB-β 1 or other molecules that promote cellular migration [16,17] and invasiveness. The 80Hz peak appears to be a result of mutations found in basal epithelial cells, squamous epithelial cells and melanocytes and these mutations may all trigger dedifferentiation of skin cells during an epithelial-mesenchyme transition (EMT).

The basic changes in the physical biomarkers of all skin cancers studied involve similar initial cellular and blood vessel changes; however, it appears that the lack of resolution of the EMT transition, leads to invasiveness that is different in each type of carcinoma.

While it appears that the new cells, blood vessels and fibrotic collagen are all found together in the tumor, there must be other changes that promote differences in invasiveness of these cancers.

EMT presents certain features that are considered as its hallmarks, including disruption of intercellular junctions, loss of cell polarity, reorganization of the cytoskeleton, and increased cell motility. Therefore, in most experimental models, epithelial (E-cadherin) and mesenchymal (N cadherin and vimentin) markers and morphological changes are examined as indicators to confirm the occurrence of EMT [16].

For example, keratin expression is routinely used by pathologists to identify epithelial-derived carcinoma cells but cannot be used to identify post-EMT cells because these cells should no longer express keratin [24]. Post-EMT epithelial cells are phenotypically like normal vimentin-expressing stromal cells. Several groups have attempted to address this issue. It has been suggested to use the term EMT like is a more descriptive and accurate term to describe the phenotypes of epithelial cancers, because it does not imply a specific mechanism, or origin of the cells described [25]. Three functional criteria to define EMT-like phenotypes in human carcinomas include: i) state of cell polarization, ii) state of cell cohesiveness, and iii) intermediate filament protein expression. [25].

Since the 80Hz peak appears to be found in the presence of the 130Hz peak in BCCs could these two peaks be a result of cellular mutations alone or are other changes to the extracellular matrix needed for these two peaks to form? Do carcinomas form because of cellular mutations alone or do they also require UV light exposure to disrupt and fragment the extracellular matrix of the papillary dermis? If both cellular mutations and disruption of the extracellular matrix were necessary for cancerous lesion formation, then this would explain the similar changes to the ECM observed by VOCT in all skin cancers as well as differences in the invasiveness and metastatic behavior seen in different types of cancer.

When one examines small lesions from patients with BCCs, there appears to be lesions with large 80Hz and 130Hz peaks in the absence of 260Hz peaks located in the papillary dermis (See Figure 2). The maximum peak values for the 80Hz and 130Hz peaks appear to coincide with each other at depths of between 0.15 and 0.35mm implying that the EMT transition causes cell migration from the epidermis to the papillary dermis. This migration is associated with formation of new blood vessels. However, formation of new fibrous tissue (260Hz peak) appears to occur after cell migration and capillary formation occurs in larger BCC lesions in the same biopsy.

If small BCC lesions are located early in their growth cycle, then it may be possible through dermoscopic, and early VOCT observations to find inhibitors of fibrosis that may block formation of the 260Hz peak limiting tumor expansion. This would provide a partial solution to limit the growing numbers of skin cancers that require excisional treatment in future decades. It is interesting to note that the fibrotic tissue deposited in all BCCs appears to surround the new cells (80Hz) and blood vessels (130Hz) as demonstrated by the Figures 2B-5B. This data suggests the invasiveness of BCCs may be limited by the fibrotic encapsulation of the tumor similar to what is seen around synthetic non-degradable implant materials. An interesting question is whether invasive and metastatic cancers like SCC and melanoma exhibit the same degrees of tumor encapsulation by fibrotic tissues as is exhibited by BCCs.

Figure 6

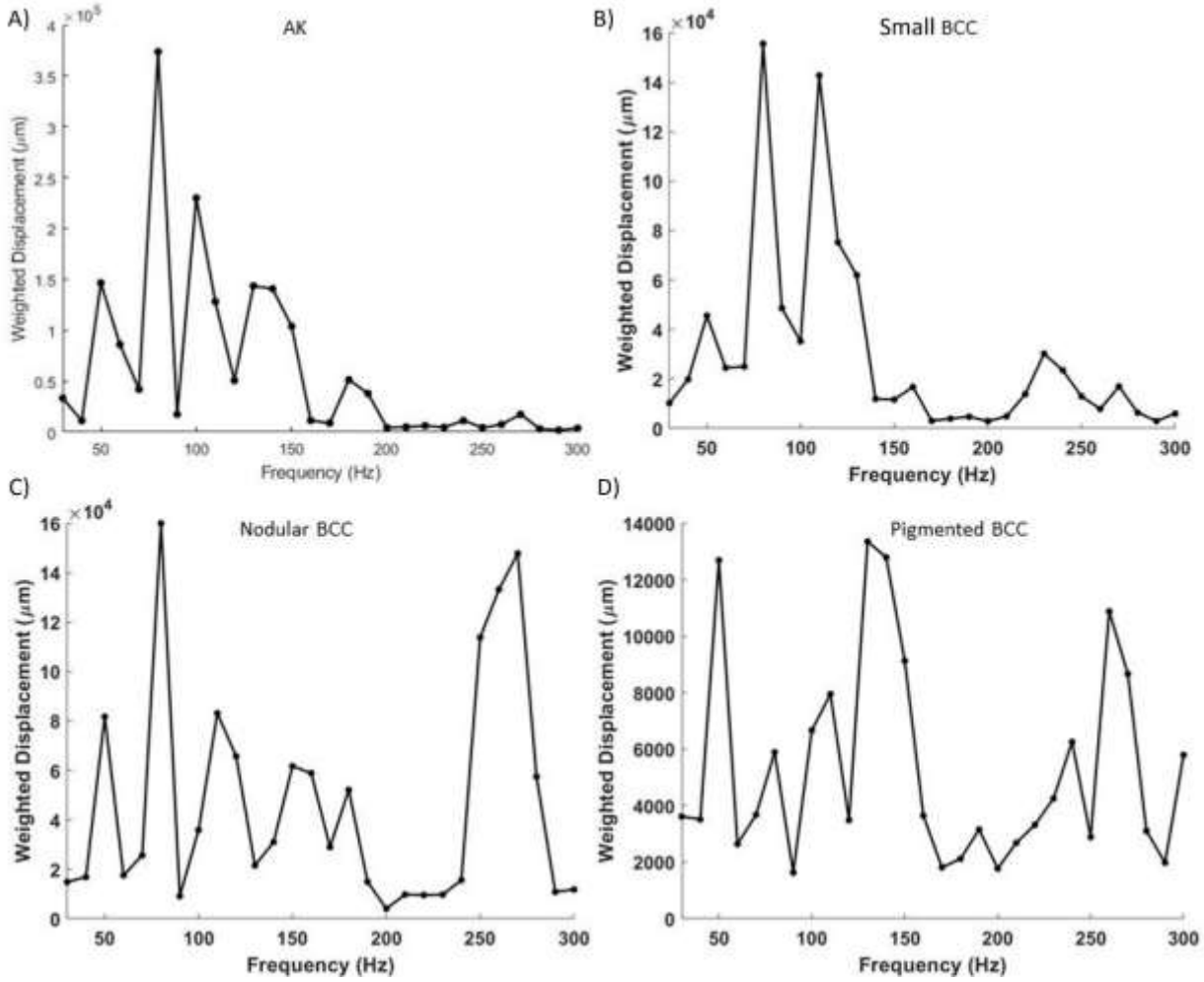

Figure 6. A plot of average cross-section 2D VOCT data shows the weighted displacement versus frequency for an actinic keratosis (A), a small cross-sectional lesion in a larger nodular BCC (B), a nodular BCC (C) and a pigmented BCC (D). Note the presence of major peaks at 50Hz, 80Hz and 130Hz peaks in the small AK (A) and the small lesion in BCC (B) while nodular BCC (C) and pigmented BCC (D) all have peaks at 50Hz, 80Hz, 130Hz, and at 260Hz. Note pigmented BCC (D) has a higher ratio of the 50 to 80Hz peak compared to the other cancerous BCC lesions. This data is an average of the 3D plots shown in Figures 2B, 3B, 4B, and 5B and illustrates the differences in the heights of the 50Hz, 80Hz and 260Hz peaks in different lesions.

5.0 Conclusions

We have measured the resonant frequency and elastic moduli of nodular, superficial, sclerotic and pigmented BCCs using a new technique termed VOCT. In very small lesions (about 0.05 mm in diameter) new 80Hz and 130Hz resonant frequency peaks are seen not present in normal skin. In all other BCCs types, new 80Hz, 130Hz and 260Hz resonant frequency peaks are found like those found in other carcinomas including SCC and melanoma. While all large BCCs were found to contain a mixture of new cells and blood vessels mixed in with fibrotic tissue in the papillary dermis, other factors must drive differences in the shape and invasiveness of the different BCCs

such as the degree of UV damage to the surrounding ECM. Pigmented BCCs exhibit a larger ratio of the 50Hz/80Hz peaks compared to the other BCC types. It is concluded that fibrotic tissue is found encapsulating all cancerous BCCs and that this layer of tissue may limit invasiveness and metastatic behavior of this tumor type.

The dense fibrotic tissue that is characteristic of all BCC skin carcinomas studied maximizes in the papillary dermis at the same depth as the 80Hz and 130Hz peaks suggesting that the new cells and blood vessels are found together with the fibrotic collagen in the tumor. While UV light destruction of the ECM may be required for fibrotic tissue deposition, cellular mutations may drive the shape and invasiveness of the final lesion. Further studies are needed to understand the factors that drive differences in shape and invasiveness of cancerous tumors.

6.0 References

1. Skin Cancer 101. Skin cancers. *Skin Cancer Found J* 2019;XXX VII:24-25.

2. Siegel RL, Miller KD, Fuchs HE, Jemal A. Cancer Statistics. CA. *Cancer J. Clin*. 2021; *71*: 7–33.

3. Lomas A, Leonardi-Bee J, Bath-Hextall F. A systematic review of worldwide incidence of nonmelanoma skin cancer. *Br. J. Dermatol.* 2012; 166:1069-1080

4. *Amercian Academy of Dermatology Association Website.* Types of skin cancer. cancer-facts-and-figures-2021.pdf.

5. Wang DM, Morgan F. Besaw RJ, Schmults CD. An ecological study of skin biopsies and skin cancer treatment procedures in the United States Medicare population. 2000 to 2015. *J Amer Acad Dermatol.* 2018; 78: 47–53.

6. Asgari MM, Moffet HH, Ray T, et al. Trends in basal cell carcinoma incidence and identification of high-risk subgroups. *J Amer Acad Dermatol.* 2015; 151: 976-981.

7. Cojocora A, Marinescu EA, Llinoui NC, Negria A, Ciurea NE. Basal Cell Carcinoma and its Impact on Different Anatomical Regions. *Curr Health Sci J.* 2021; 47: 75–83.

8. Jee BA, Lim H, Kwon SM, Jo Y, Park MC, Lee IJ, Woo HG. Molecular classification of basal cell carcinoma of skin *by* gene expression profiling. *Mol Carcinog.* 2015; 54:1605–1612.

9. Emiroglu N, Cengiz FP, Kemerliz F. The relationship between dermoscopy and histopathology of basal cell carcinoma. *An. Bras. Dermatol*. 2015; 90: 351-356.

10. Dourmishev LA, Rusinova D, Botev I. Clinical variants, stages, and management of basal cell carcinoma. *Indian Dermatol Online J* 2013; 4:12-7.

11. Lupu M, Caruntu C, Popa MI, et al. Vascular patterns in basal cell carcinoma: Dermoscopic, confocal and histopathological perspectives. *Oncol. Lett.* 2019; 17:4112-4125.

12. Schuh S, Holmes J, Ulrich M, et al. Imaging blood vessel morphology in skin: dynamic optical coherence tomography as a novel potential diagnostic tool in dermatology. *Derm Ther (Heidelb)*. 2017; 7:187-202.

13. Paolino G, Donati M, Didona D, Mercuri SR, Cantisani C. Histology of Non-Melanoma Skin Cancers: An Update. *Biomedicines* 2017: 71; doi:10.3390/biomedicines5040071.

14. Rohani P, Yaroslavsky AN, Feng X, Jermain P, Shaath T, Neel VA. Collagen disruption as a marker for basal cell carcinoma in presurgical margin detection. *Lasers Surg Med*. 2018; 50:902-907.

15. Silver FH, Deshmukh T, Benedetto D, Kelkar N. Mechano-vibrational spectroscopy of skin: Are changes in collagen and vascular tissue components early signs of basal cell carcinoma formation? *Skin. Res. Technol*. 2020; 27:227–233.
16. Silver FH, Kelkar N, Deshmukh T, Ritter K, Ryan N, Nadiminiti H. Characterization of the biomechanical properties of skin using vibrational optical coherence tomography: Do changes in the biomechanical properties of skin stroma reflect structural changes in the extracellular matrix of cancerous lesions? *Biomolecules* 2021; 11: 1712. https://doi.org/10.3390/ biom11111712.
17. Silver FH, Deshmukh T, Kelkar N , Ritter N, Nicole Ryan, and Nadiminti N. The "Virtual Biopsy" of Cancerous Lesions in 3D: Non-Invasive Differentiation between Melanoma and Other Lesions Using Vibrational Optical Coherence Tomography. *Dermatopathology* 2021; 8:539–551. https://doi.org/ 10.3390/dermatopathology8040058.
18. Silver FH, Shah RG, Richard M, Benedetto D. Comparative "virtual biopsies" of normal skin and skin lesions using vibrational optical coherence tomography. *Skin. Res. Technol*. 2019; *25*:743–749.
19. Silver FH, Shah RG, Richard M, Benedetto D. Use of Vibrational Optical Coherence Tomography to Image and Characterize a Squamous Cell Carcinoma. *J. Dermatology Res. Ther.* 2019; *5*: 1–8.
20. Silver FH. Measurement of Mechanical Properties of Natural and Engineered Implants. *Adv. Tissue Eng. Regen. Med.* Open Access 2016; 1: 20–25.
21. Shah, R.G.; Devore, D.; Pierce, M.C.; and Silver, F.H.; Vibrational analysis of implants and tissues: Calibration and mechanical spectroscopy of multi-component materials. *J. Biomed. Mater. Res. - Part A* 2017, *105*, 1666–1671.
22. Silver, F.H.; Kelkar, N.; Desmukh, T.; Horvath, I.; Shah, R.G.; Mechano-Vibrational Spectroscopy of Tissues and Materials Using Vibrational Optical Coherence Tomography: A New Non-Invasive and Non-Destructive Technique. *Recent Progress in Materials* 2020, 2, doi:10.21926/rpm.2002010.
23. Shah, R.G.; Silver, F.H.; Viscoelastic Behavior of Tissues and Implant Materials : Estimation of the Elastic Modulus and Viscous Contribution Using Optical Coherence Tomography and Vibrational Analysis. *J. Biomed. Technol. Res.* 2017, *3*, 1–5.
24. Barak V, Goike H, Panaretakis KW, Einarsson R: Clinical utility of cytokeratins as tumor markers. *Clin Biochem* 2004, 37:529 – 540
25. Klymkowsky MW, Savagner P. Epithelial-Mesenchymal Transition A Cancer Researcher's Conceptual Friend and Foe. *Am J Pathol* 2009, 174:1588 –1593; DOI: 10.2353/ajpath.2009.080545)

